Electronic Supplementary Material (ESI) for Catalysis Science & Technology.

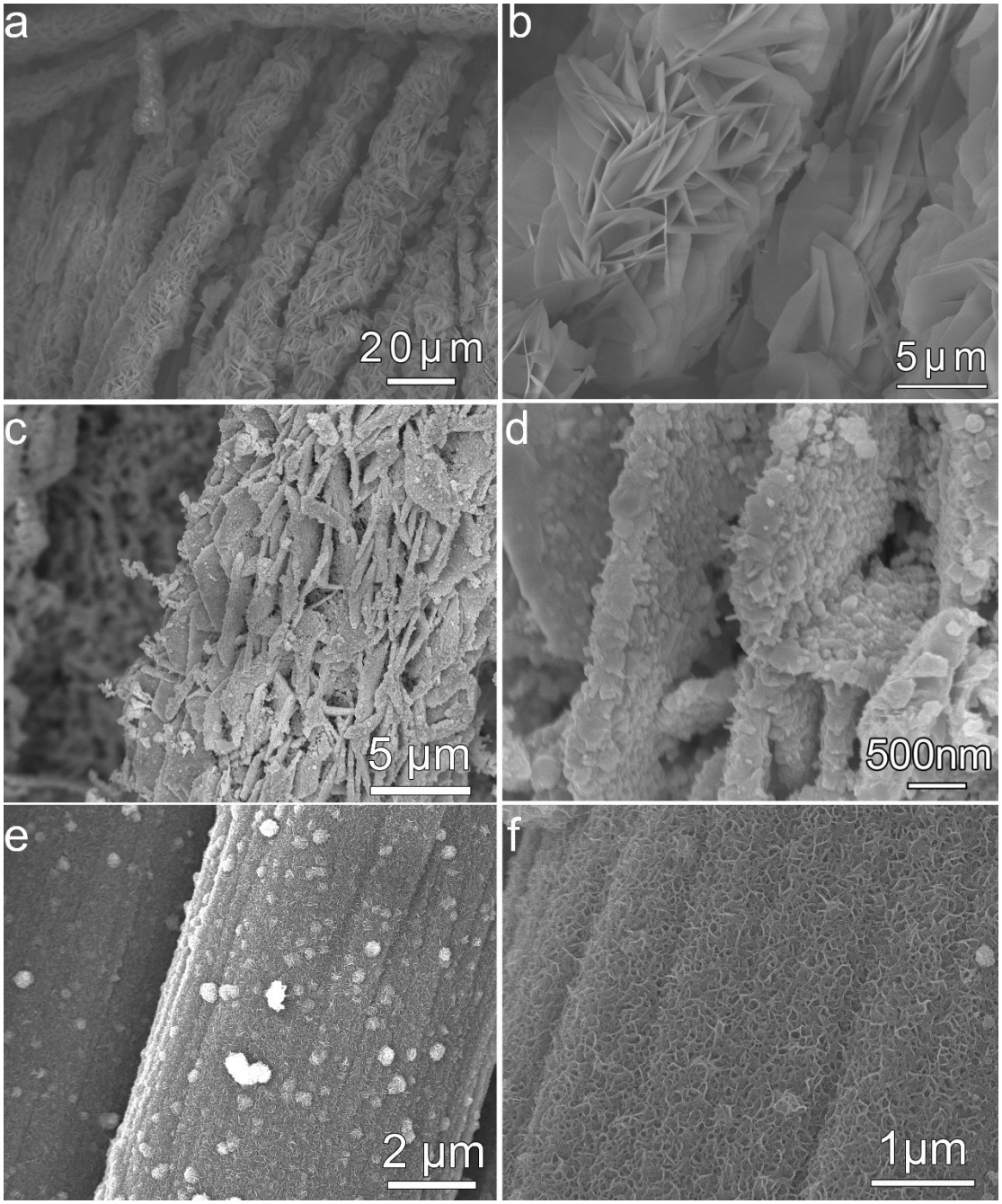

Figure S1. SEM image of (a, b) $Ni(OH)_2$/CC, (c, d) Ni_3S_4/CC, (e, f) 1T-MoS_2/CC.

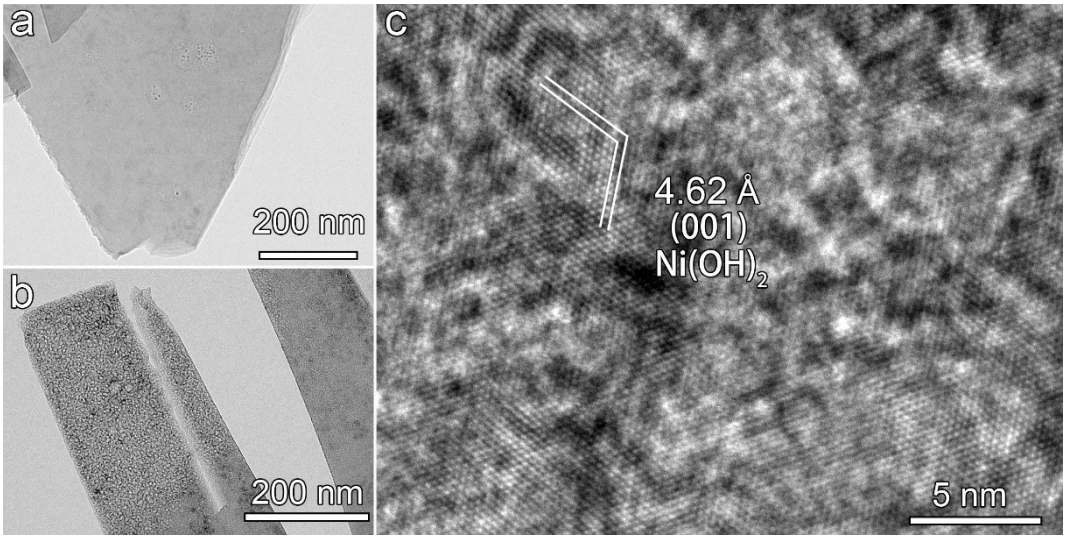

Figure S2. TEM image of Ni $(OH)_2$/CC.

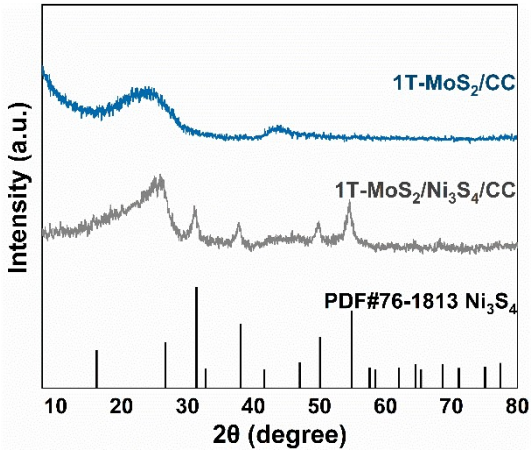

Figure S3. The XRD pattern of 1T-MoS_2 /CC and 1T-MoS_2/Ni_3S_4/CC.

The XRD pattern shown that no distinct peaks for 1T-MoS_2 were observed, indicating that the 1T-MoS_2 in both catalysts has a poor crystallinity.

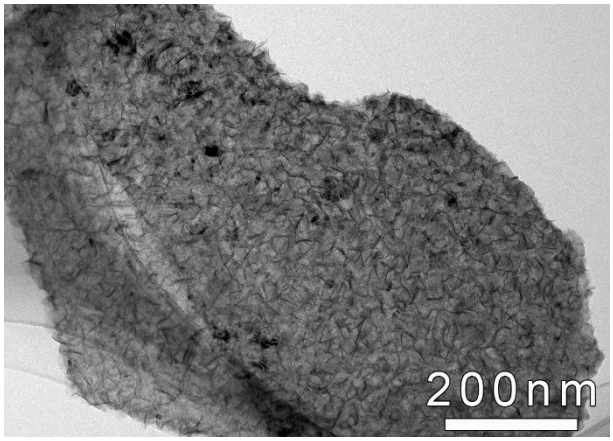

Figure S4. TEM image of 1T-MoS_2/Ni_3S_4/CC.

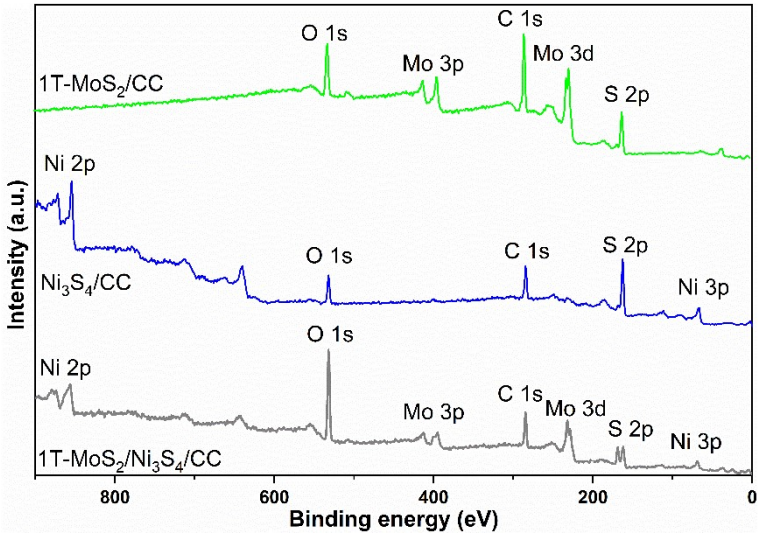

Figure S5. XPS survey of 1T-MoS_2/CC, Ni_3S_4/CC and 1T-MoS_2/Ni_3S_4/CC.

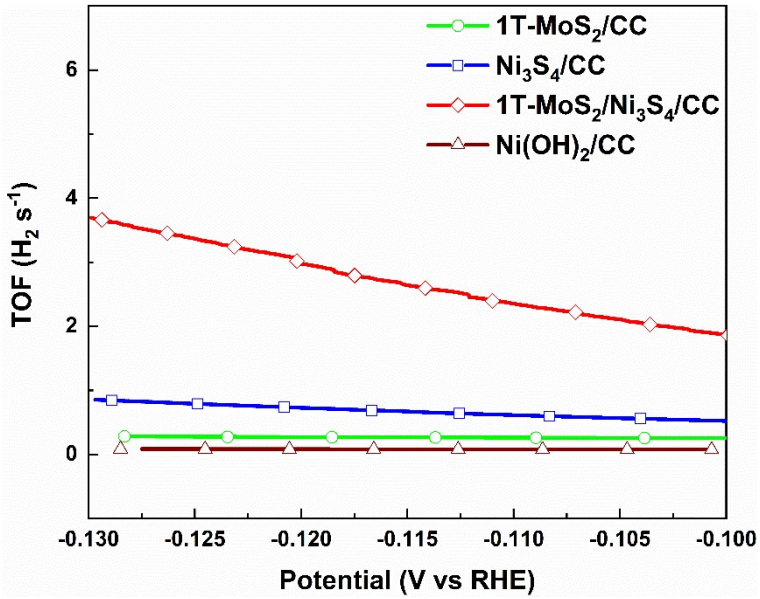

Figure S6. The TOF of 1T-MoS_2/CC, Ni_3S_4/CC, Ni $(OH)_2$/CC and 1T-MoS_2/Ni_3S_4/CC.

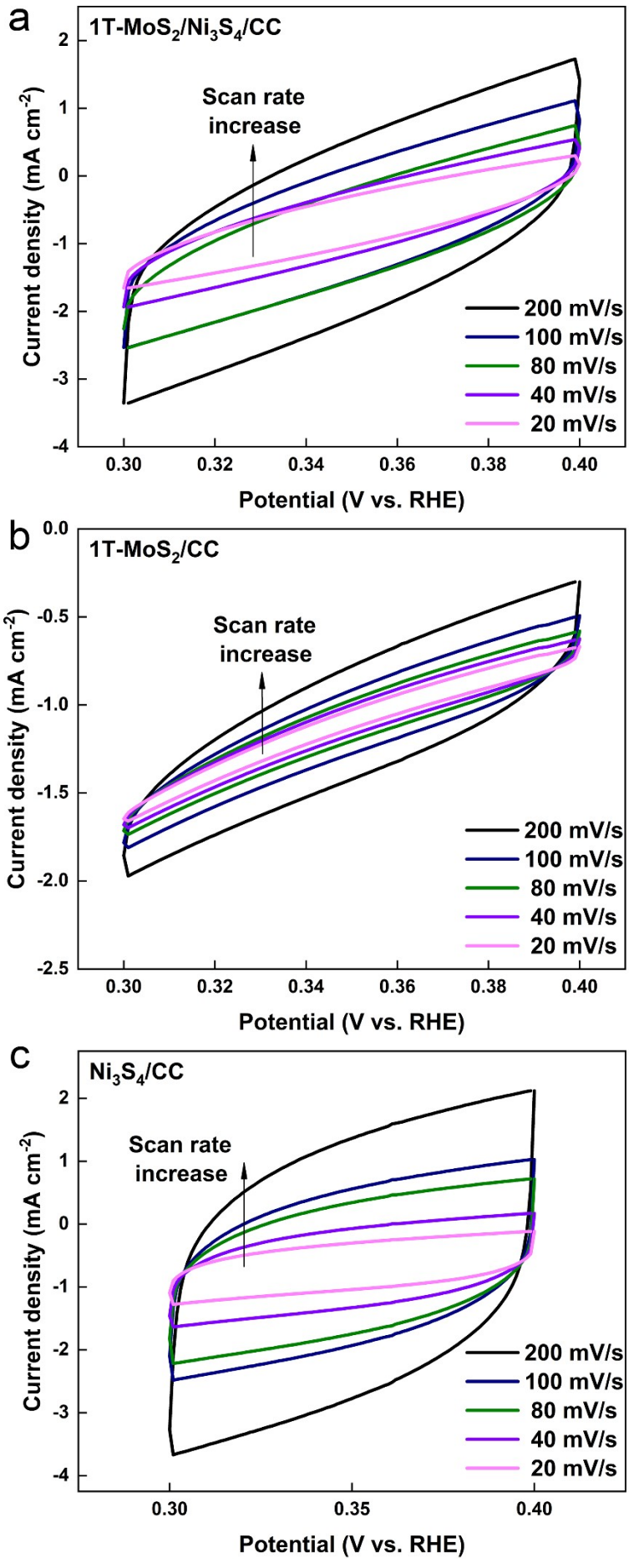
a
1T-MoS2/Ni3S4/CC
Scan rate increase
Current density (mA cm-2)
Potential (V vs. RHE)
200 mV/s
100 mV/s
80 mV/s
40 mV/s
20 mV/s
b
1T-MoS2/CC
Scan rate increase
Current density (mA cm-2)
Potential (V vs. RHE)
200 mV/s
100 mV/s
80 mV/s
40 mV/s
20 mV/s
c
Ni3S4/CC
Scan rate increase
Current density (mA cm-2)
Potential (V vs. RHE)
200 mV/s
100 mV/s
80 mV/s
40 mV/s
20 mV/s

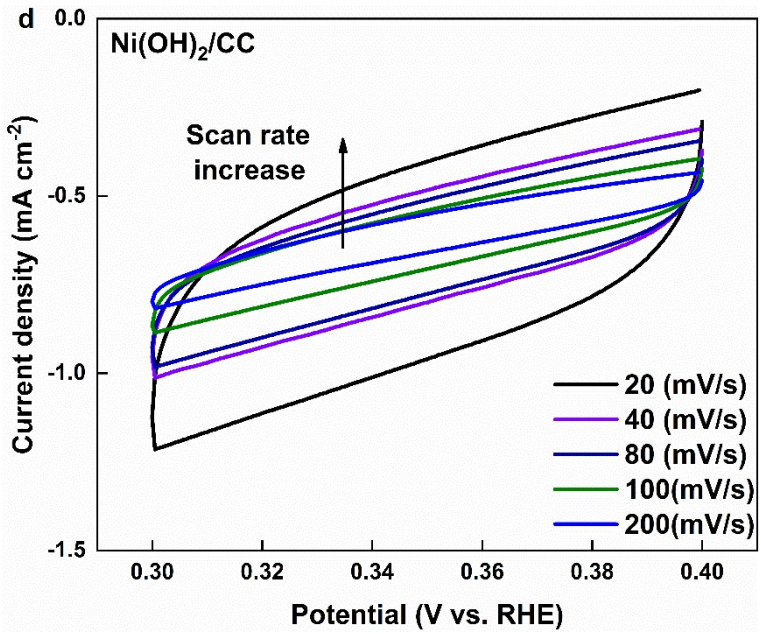

Figure S7. CV cycles at scan rates ranging from 20 mV s^{-1} to 200 mV s^{-1} of (a) 1T-MoS_2/Ni_3S_4/CC, (b) 1T-MoS_2/ CC, (c) Ni_3S_4/CC and (d) Ni $(OH)_2$/CC.

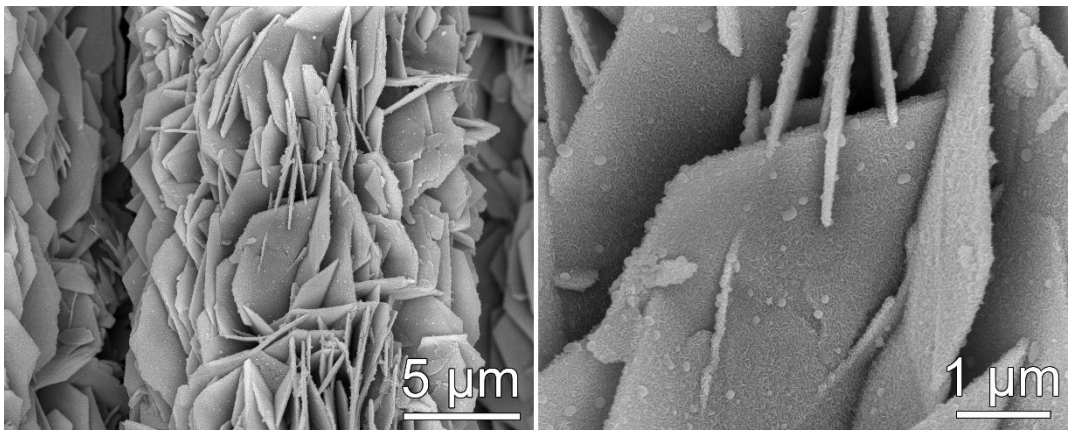

Figure S8. SEM image of 1T-MoS_2/Ni_3S_4/CC after 40 h chronoamperometry test.

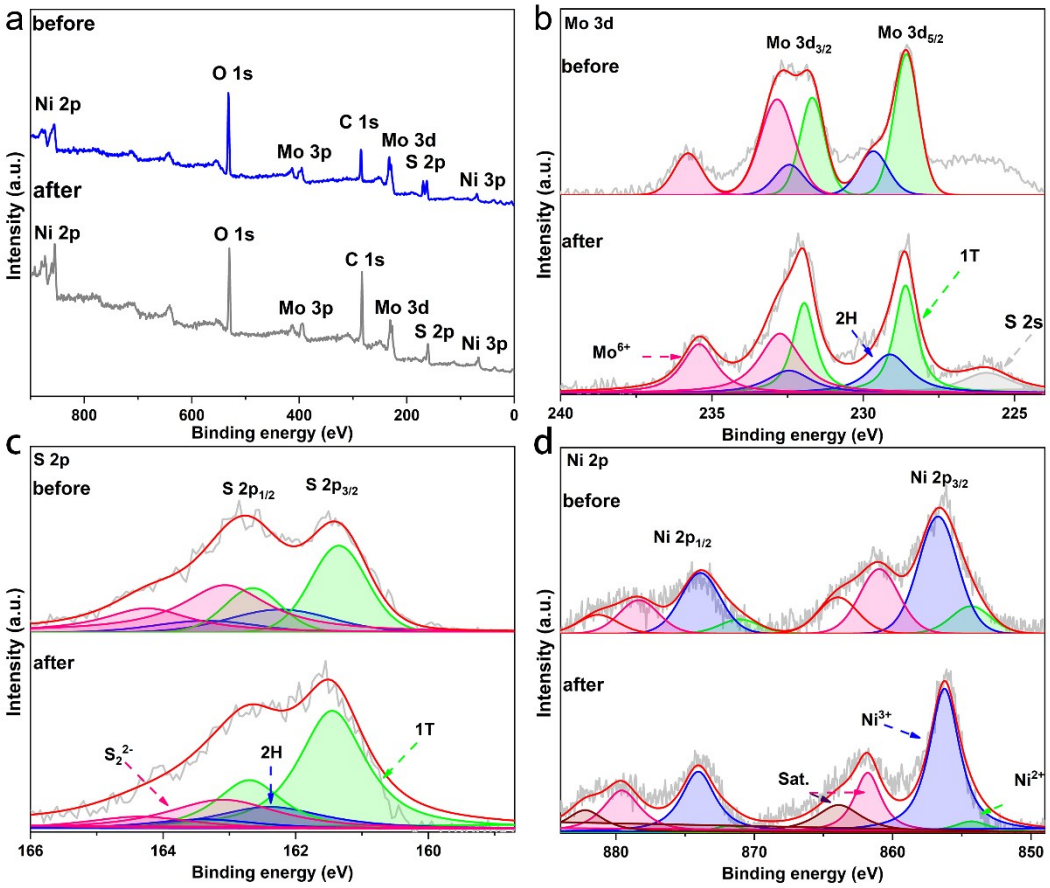

Figure S9. XPS of 1T-MoS_2/Ni_3S_4/CC before and after 40 h chronoamperometry test. (a) Survey spectrum, and high-resolution spectra of (b) Mo 3d, (c) S 2p, and (d) Ni 2p.

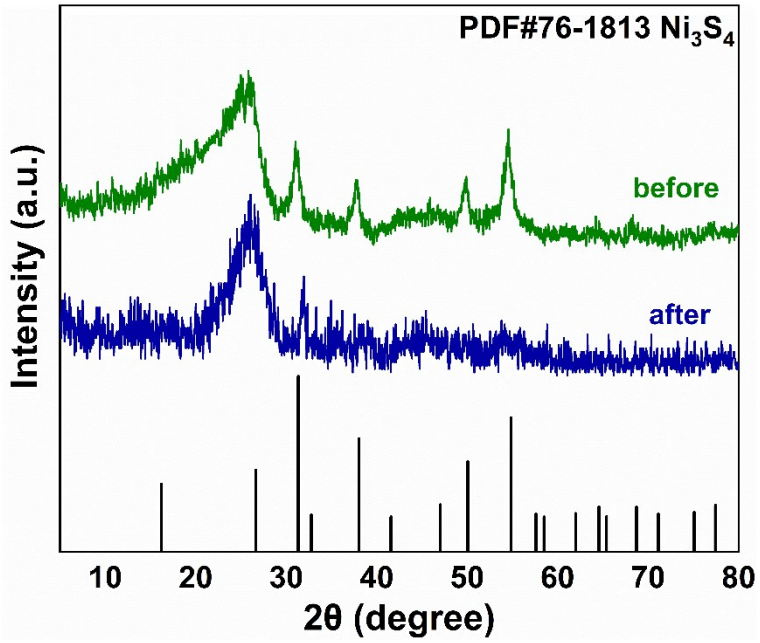

Figure S10. The XRD pattern of 1T-MoS_2/Ni_3S_4/CC before and after 60 h chronoamperometry test.

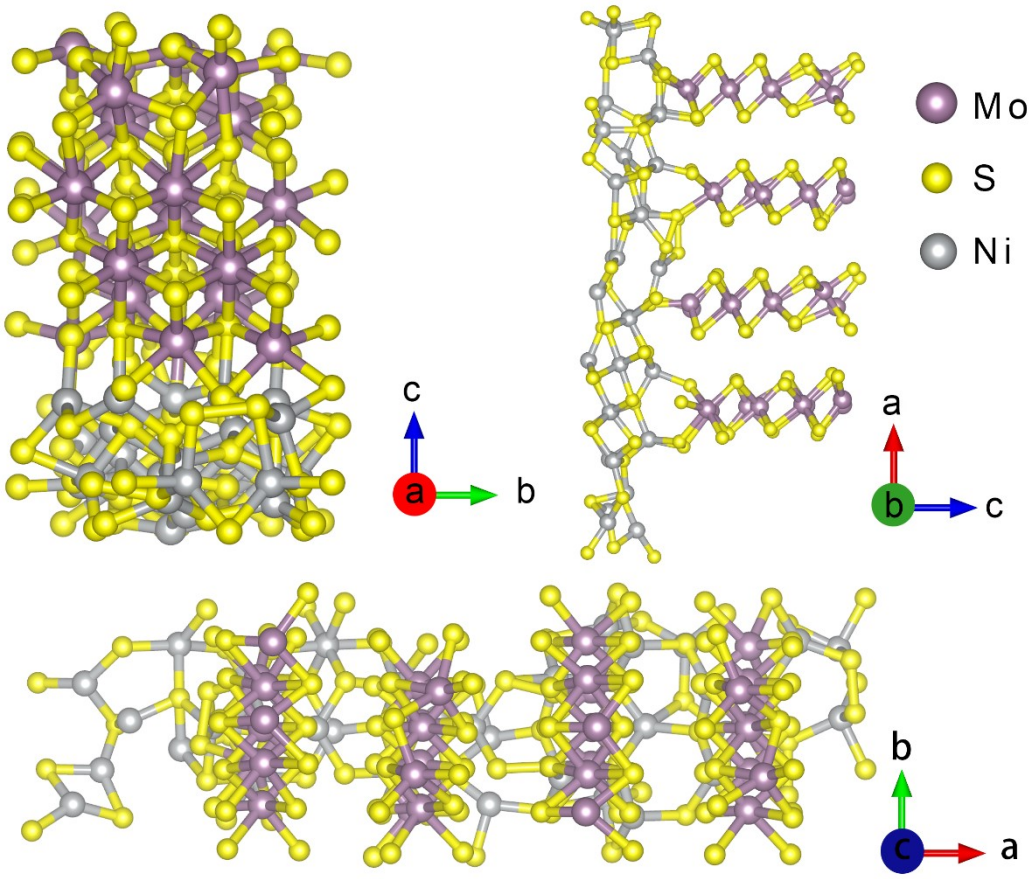

Figure S11. The optimal structure model of 1T-MoS_2/Ni_3S_4.

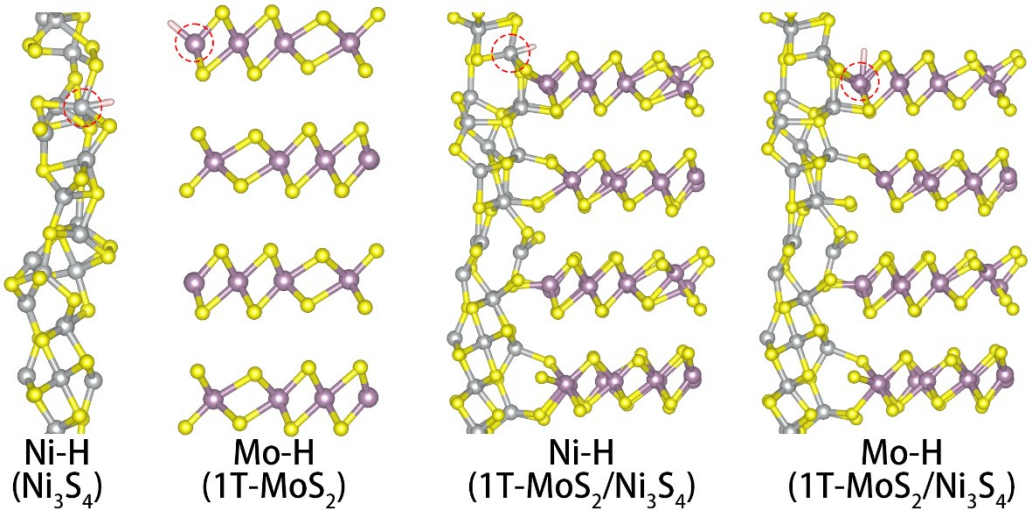

Figure S12. Structural models for hydrogen adsorption on Ni sites (Ni_3S_4), Mo-edge sites (1T-MoS_2), Ni and Mo-edge sites (1T-MoS_2/Ni_3S_4).

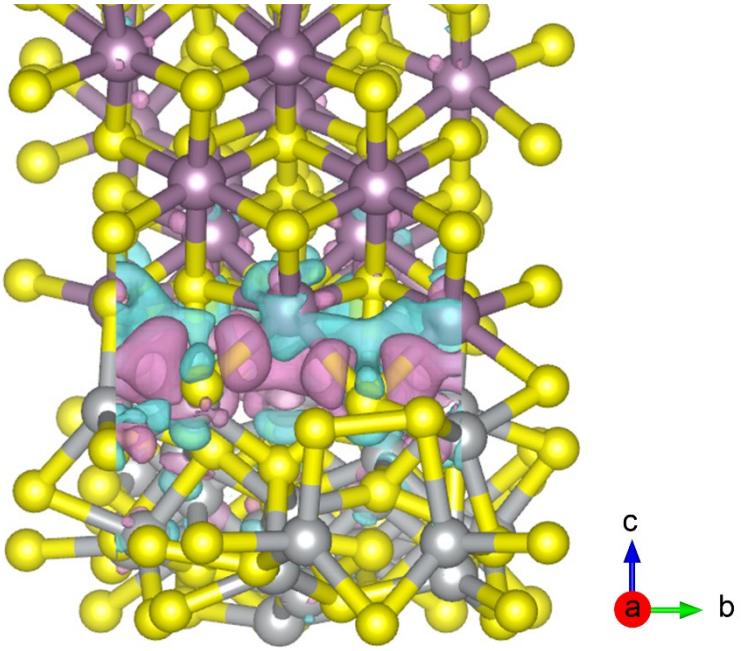

Figure S13. The deformation of the electronic density of 1T-MoS_2/Ni_3S_4 interfaces, in which the cyan/purple is surfaces correspond to negative/ positive spin densities.

Table S1. The loading of the catalytically active substance on the carbon cloth calculated from ICP-OES results.

Sample	Element	Concentration (mg/L)	Loading (mg/cm^2)
MoS_2/Ni_3S_4	Mo	0.41	0.41
	Ni	0.35	0.35
	S	1.42	1.42
$Ni(OH)_2$	Ni	2.16	2.16

Table S2. A comparison of the catalytic performance of 1T-MoS_2/Ni_3S_4/CC and recently reported MoS_2-based HER catalysts in 1.0 M KOH.

Samples	η_{10} (mV)	Tafel slope	Ref.

		(mV dec^{-1})	
1T-MoS_2/Ni_3S_4/CC	44	44	This work
MoS_2/α-MoC	84	41	[1]
1T-2H MoS_2/CoS_2	37	46	[2]
Ni-1T-MoS_2	199	53	[3]
NiO@1T-MoS_2	46	52	[4]
P-1T-CMS@CC	95	69	[5]
Co-MoS_2/V_2C@CC	70	99	[6]
Cu-MoS_2@NF	72	68	[7]
$Ni(OH)_2$@1T-MoS_2 NWAs	57	70	[8]
N-rGO-MoS_2-$Ni(OH)_2$	129	86	[9]
CoS_2-MoS_2 MSHSs	109	52	[10]
MoS_2/NiS_2	62	50	[11]
CoMoNiS-NF-31	113	85	[12]
(Ni, Fe)S_2@MoS_2	130	101	[13]
Co-MoS_2/BCCF-21	48	52	[14]
Co_3S_4@MoS_2	136	43	[15]
CoMoS	97	70	[16]
2.5H-PHNCMs	70	38	[17]
FeCoNi-HNTAs	58	38	[18]
MoS_2-Ni_3S_2/NF	98	61	[19]
MoS_2/Ni_3S_2@NF	110	83	[20]

Reference

1. Z. Cheng, Y. Xiao, W. Wu, X. Zhang, Q. Fu, Y. Zhao and L. Qu, ACS Nano, 2021, 61, 20210702.
2. P. Chang, T. Wang, Z. Liu, X. Wang, J. Zhang, H. Xiao, L. Guan and J. Tao, J. Mater. Chem. A, 2022, 10, 16115-16126.
3. G. Wang, G. Zhang, X. Ke, X. Chen, X. Chen, Y. Wang, G. Huang, J. Dong, S. Chu and M. Sui, Small, 2022, 18, e2107238.
4. Y. Huang, Y. Sun, X. Zheng, T. Aoki, B. Pattengale, J. Huang, X. He, W. Bian, S. Younan, N. Williams, J. Hu, J. Ge, N. Pu, X. Yan, X. Pan, L. Zhang, Y. Wei and J. Gu, Nat. Commun., 2019, 10, 982.
5. C. C. Gudal, U. N. Pan, D. R. Paudel, M. R. Kandel, N. H. Kim and J. H. Lee, ACS Appl. Mater. Inter., 2022, 14, 14492-14503.
6. Y. Chen, G. Meng, T. Yang, C. Chen, Z. Chang, F. Kong, H. Tian, X. Cui, X. Hou and J. Shi, Chem. Eng. J., 2022, 450, 138157.
7. B. Gao, Y. Zhao, X. Du, Y. Chen, B. Guan, Y. Li, Y. Li, S. Ding, H. Zhao, C. Xiao and Z. Song, J. Mater. Chem. A, 2021, 9, 8394-8400.
8. K. Wang, Z. Liu, Q. Gao, N. Li and K. Yu, Appl. Surf. Sci., 2022, 593, 153408.
9. S. Debata, S. Banerjee and P. K. Sharma, Electrochim. Acta, 2019, 303, 257-267.
10. V. Ganesan and J. Kim, Int. J. Hydrogen Energ., 2020, 45, 13290-13299.

11. J. Lin, P. Wang, H. Wang, C. Li, X. Si, J. Qi, J. Cao, Z. Zhong, W. Fei and J. Feng, Adv. Sci., 2019, 6, 1900246.
12. Y. Yang, H. Yao, Z. Yu, S. M. Islam, H. He, M. Yuan, Y. Yue, K. Xu, W. Hao, G. Sun, H. Li, S. Ma, P. Zapol and M. G. Kanatzidis, J Am. Chem. Soc., 2019, 141, 10417-10430.
13. Y. Liu, S. Jiang, S. Li, L. Zhou, Z. Li, J. Li and M. Shao, Appl. Catal. B-Environ., 2019, 247, 107-114.
14. Q. Xiong, Y. Wang, P. F. Liu, L. R. Zheng, G. Wang, H. G. Yang, P. K. Wong, H. Zhang and H. Zhao, Adv. Mater., 2018, 15, e1801450.
15. Y. Guo, J. Tang, Z. Wang, Y.-M. Kang, Y. Bando and Y. Yamauchi, Nano Energy, 2018, 47, 494-502.
16. J. Hou, B. Zhang, Z. Li, S. Cao, Y. Sun, Y. Wu, Z. Gao and L. Sun, ACS Cata., 2018, 8, 4612-4621.
17. H. Li, S. Chen, Y. Zhang, Q. Zhang, X. Jia, Q. Zhang, L. Gu, X. Sun, L. Song and X. Wang, Nat. Commun., 2018, 9, 2452.
18. H. Li, S. Chen, X. Jia, B. Xu, H. Lin, H. Yang, L. Song and X. Wang, Nat. Commun., 2017, 8, 15377.
19. Y. Yang, K. Zhang, H. Lin, X. Li, H. C. Chan, L. Yang and Q. Gao, ACS Cata., 2017, 7, 2357-2366.
20. J. Zhang, T. Wang, D. Pohl, B. Rellinghaus, R. Dong, S. Liu, X. Zhuang and X. Feng, Angew Chem. Int. Ed. Engl., 2016, 55, 6702-6707.